



CONTINUING EDUCATION PROGRAM: FOCUS...

Tips and traps in neurological imaging: Imaging the perimedullary spaces

J.-L. Dietemann*, A. Bogorin, M. Abu Eid, R. Sanda, I. Mourao Soares, S. Draghici, N. Rotaru, M. Koob

Department of Radiology 2, hôpital de Hautepierre, hôpitaux universitaires de Strasbourg, avenue Molière, 67098 Strasbourg cedex, France

KEYWORDS

Spine;
Spinal cord;
Artifacts;
Veins;
Epidural fat

Abstract The spinal canal is frequently a source of difficulties, traps and diagnostic errors. Pitfalls related to artifacts are resolved by using appropriate sequences. Good knowledge of the appearance of certain particular anatomical structures (the cauda equina roots, the radicular veins of the lumbar spine and conus medullaris, the dorsal root ganglion) and of frequent variants (fibrolipoma of the filum terminale, common root sheaths, root cysts) will avoid a good many errors. Dilatation of epidural veins in intracranial hypotension can simulate the contrast enhancement of a tumour. An increase in epidural fat can induce pathogenic stenosis of the dural sheath.

© 2012 Éditions françaises de radiologie. Published by Elsevier Masson SAS. All rights reserved.

A great number of pitfalls are encountered when exploring the spinal canal in MRI, particularly around the perimedullary subarachnoid space, the spinal nerve roots, root sheaths and the epidural space. Some of them are related to anatomical variations, rare diseases or unusual signs, others to artifacts or the use of inappropriate exploratory protocols.

The subarachnoid space and the CSF

The quality of MRI explorations of the CSF of the subarachnoid space in the spinal canal is often modified by flow artifacts. These artifacts are related to CSF flow and are particularly common in the thoracic spine, especially in children, where they almost always appear. These artifacts are most often visualised on sagittal T2-weighted images in the retromedullary subarachnoid space of the thoracic spine, but also in a perimedullary distribution at the level of the cervico-thoracic junction, appearing as areas devoid of any signal; on spin echo axial slices these artifacts often surround the entire spinal cord ('black

* Corresponding author.

E-mail address: jean-louis.dietemann@chru-strasbourg.fr (J.-L. Dietemann).

holes') (Figs. 1 and 2). These modifications are sometimes confused with extramedullary intradural tumoral processes or vascular dilatations in the context of an arteriovenous malformation (AVM) [1]. The differential diagnosis with an AVM is easy, because perimedullary vascular dilatations associated with an angioma are either discreet, located directly in contact with the posterior medullary surface and associated with an intramedullary high intensity signal on T2 related to edema of venous origin, if there is a dural fistula, in the adult, or larger and associated with intramedullary vascular dilatation if there is an AVM of the spinal cord in the child. Flow artifacts are virtually non-existent in the lumbar region and can be avoided on axial T2 images of the cervical and thoracic spine using axial slices in a MEDIC or MERGE T2 gradient echo sequence; moreover, with such sequences the intramedullary signal can be closely studied because they are the only ones to offer good discrimination between the white and the grey matter. Flow artifacts are also reduced using BLADE sequences [2].

The retromedullary subarachnoid space of the thoracic spine presents a high degree of trabeculation, the trabeculae appearing more distinctly on the median line where they may form the septum posticum which attaches the posterior surface of the spinal cord to the dural sheath; this median sagittal septum can be identified on high resolution T2-weighted axial images.

Magnetic susceptibility artifacts can simulate compression of the dural sheath; these artifacts are observed postoperatively, particularly following discectomy, associated or not with arthrodesis, via an anterior approach. These artifacts are accentuated on axial T2 gradient-echo images but are less important in spin echo (Fig. 3).

3D SPACE or CUBE T2-weighted spin echo sequences are less sensitive to flow artifacts and magnetic susceptibility, enabling the root sheaths to be properly studied and clearly seen along their subarachnoid pathway, complementing 3D CISS or FIESTA T2 sequences. However these sequences



Figure 2. Anterior cervical premedullary and posterior thoracic flow artifacts at 3 T.

cannot be used to analyse the signal in the spinal cord; if there are clinical spinal cord symptoms, these sequences can consequently only be used as an addition to basic sequences (sagittal slices in 2D T2-weighted fast spin echo and MEDIC or MERGE axial slices). Moreover, T2 SPACE or CUBE images are often associated with an artifact on the surface of the spinal cord appearing as a fine low intensity border separating the spinal cord from the CSF and which may simulate siderosis of the spinal cord (Fig. 4).

The anterior and posterior cervical, thoracic and lumbar roots can be visualised on axial T2-weighted images and

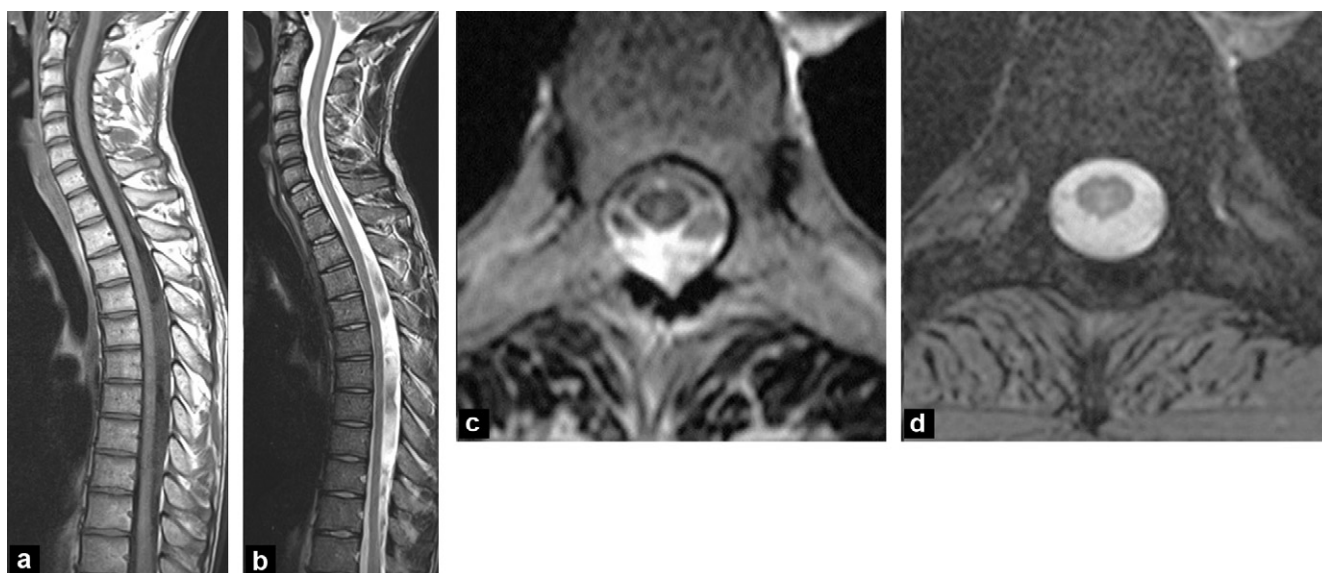


Figure 1. a–d: flow artifacts. Sagittal MRI images in T1 weighting (a) and T2 weighting (b) and axial T2-weighted spin echo (c) show very low intensity zones in T1 and T2 weighting that can simulate vascular or tumoral diseases. The artifacts disappear in axial T2-weighted gradient-echo MEDIC images (d).



Figure 3. a, b: false postoperative compression of the dural sheath on an axial T2-weighted gradient-echo image (a), owing to a magnetic susceptibility artefact. The sagittal T2-weighted fast spin echo image (b) shows no compression.

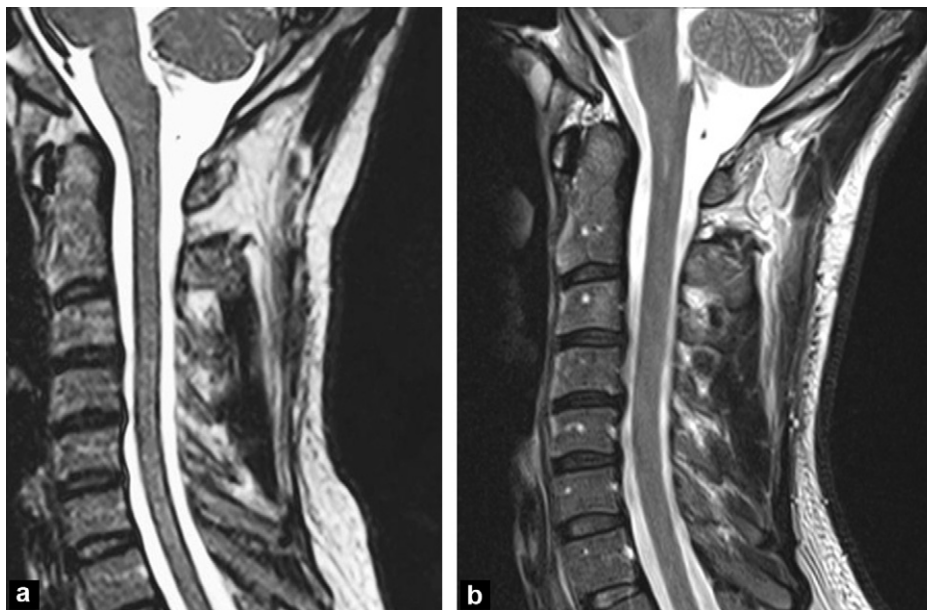


Figure 4. a, b: artifact-simulating siderosis of the spinal cord seen on a sagittal T2-weighted SPACE sequence (a). In the T2-weighted spin echo image (b), the abnormality has disappeared.

more particularly on high resolution 3D T2 imaging (CISS, FIESTA, SPACE, CUBE). Visualising the rootlets composing each cervical and thoracic root is however still a matter of chance. Frequently anastomoses between the cervical roots exist (which explains the inconsistency between the clinical symptoms and the topography of the lesions identified by imaging). In the lumbar region, the normal roots of the cauda equina present a V-shaped arrangement open towards the front on axial T2-weighted images [3]. The anterior motor component is clearly identified relative to the posterior sensory root, which appears wider. Disappearance of this V shape is either related to compression,

which is located sometimes at a distance, or to adherence phenomena related to arachnoiditis.

The dorsal root ganglion is identified using a high-resolution T2-weighted sequence (CISS, FIESTA). Intense contrast enhancement is observed following Gadolinium injection and appears very clearly when the fat signal is saturated. This nodular intraforaminal uptake must not be confused with a tumoral process, particularly a neurinoma [3,4] (Fig. 5). The dorsal root ganglion may be enlarged in cases of polyradiculoneuropathy [5].

Fibrolipoma of the filum terminale is a frequent normal variant (4% lumbar MRI examinations) and is seen as a high

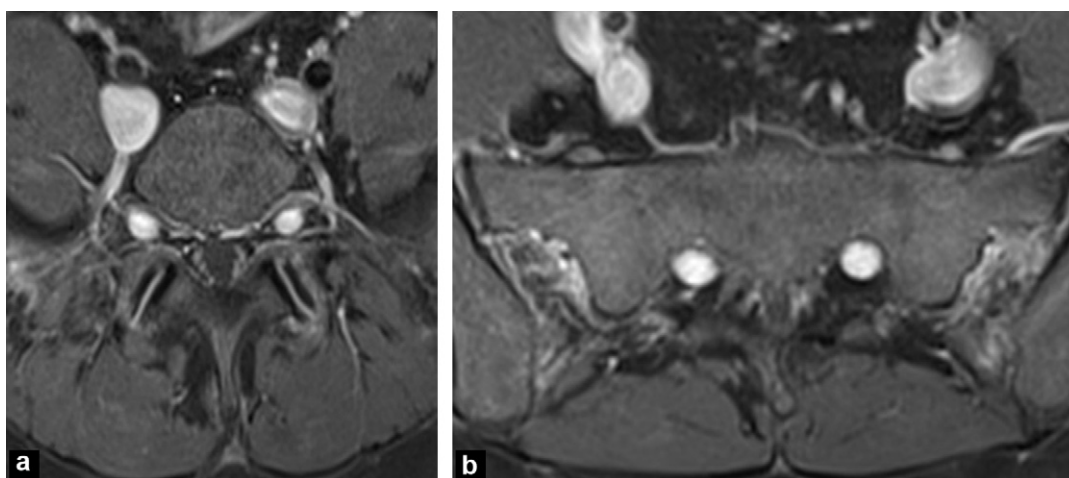


Figure 5. a, b: T1-weighted image with Gadolinium showing the normal dorsal root ganglion at L5 (a) and S1 (b).

intensity linear signal on its pathway. The high intensity signal in T2 weighting and signal drop in T1 weighting with fat saturation confirm the fatty composition of the lesion; the absence of clinical symptoms, topographical or morphological abnormalities of the conus medullaris or filum terminale, and lack of spinal dysraphia confirm that it is a normal variant [6,7] (Fig. 6).

In T1 weighting following injection of Gadolinium, MRI frequently reveals normal arterial and/or venous structures on the surface of the spinal cord, especially near the conus medullaris and on the posterior surface of the mid-thoracic cord. The veins draining the conus medullaris accompany the roots L1, L2 or L3 of the cauda equina. Radicular arteries or veins may accompany the roots L5 or S1 over their entire intradural route between the conus and the lumbosacral region (Fig. 7). In axial T1-weighted images after Gadolinium injection, this vascular contrast enhancement should not be confused with enhancement due to inflammation [8].

The spinal nerves and their sheaths

The motor and sensory roots of the cervical spinal nerves are composed of numerous rootlets. The existence of anastomoses between adjacent roots explains inconsistencies between clinical findings and imaging data: these anatomic variations cannot currently be analysed by imaging. It is also the case of the dentate ligament, which anchors the lateral surface of the spinal cord to the dural envelope between the sensory and motor roots.

There are many variations of the root sheaths that form the foraminal extension of the meningeal envelope and which thus permit the motor and sensory roots to leave the dural sheath and unite to form the spinal nerve. We will presently discuss those involved in certain differential and aetiological diagnoses, namely common sheaths and root cysts.

Common sheaths are normal at levels L4-L5 and L5-S1 with a common sheath for the roots L5 and S1 and S1 and

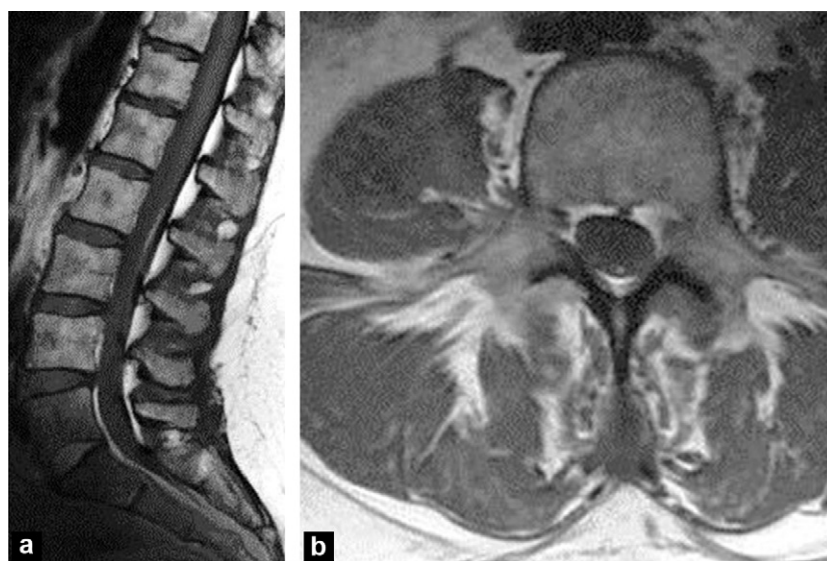


Figure 6. a, b: fibrolipoma of the filum terminale. A high intensity signal is identified at L2-L3 on a sagittal T1-weighted (a) and axial T1-weighted (b) image.

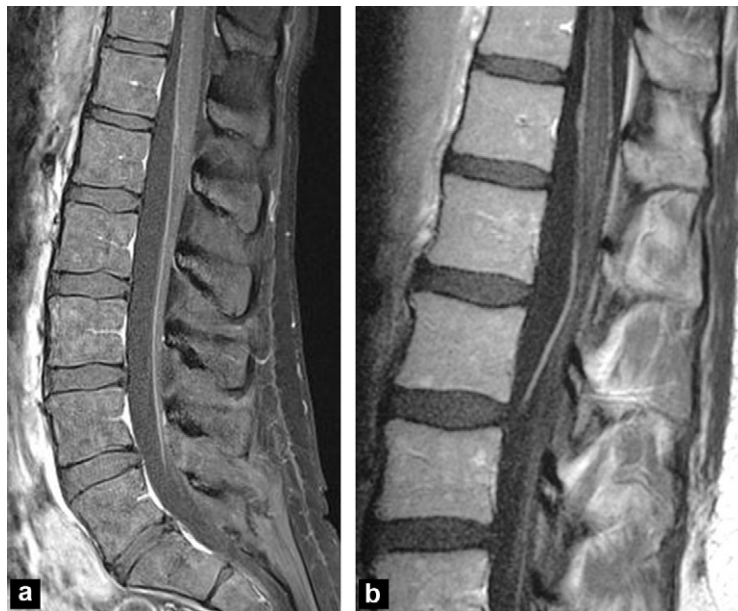


Figure 7. a, b: normal venous contrast enhancement of an L5 radicular vein (a) and a vein of the conus medullaris at L3 (b).

S2 respectively. The presence of a common L5-S1 sheath on one side and a common S1-S2 sheath contralaterally is possible. On a CT scan, but sometimes also in MRI, a common sheath can simulate disc herniation in a root recess or a foramen. The root recess is normally enlarged if there is a common sheath [9,10] (Fig. 8). Using axial T2-weighted MRI sequences up to four roots can often be identified within a single sheath. Postoperatively, enhancement of fibrosis around a dilated sheath can simulate recurrence of disc herniation with a free fragment.

Root cyst type formations occur frequently and may indicate dilatation of the root sheath, actual root cysts or Tarlov cysts (Figs. 9–11). Dilatation of root sheaths can be observed

in the lower cervical region or at the L5, S1 or S2 levels. Meningeal root cysts have a dural or arachnoid wall. These cysts are common in the lower cervical region, at the thoracolumbar junction and in the lower lumbar and sacral region. Rupture of these cysts causes a chronic leak of CSF, responsible for 'spontaneous' intracranial hypotension [11]. It is easy to identify these cysts on coronal T2 STIR or high-resolution 3D T2 images. They are associated with signs of CSF leakage and hypotension within the dural sheath (epidural and/or sub-dural fluid collection, dilatation of the epidural veins at the C1-C2 levels and in the thoracic and lower lumbar regions). If there are intracranial hypotension complications (a chronic sub-dural haematoma, cerebral involvement) and

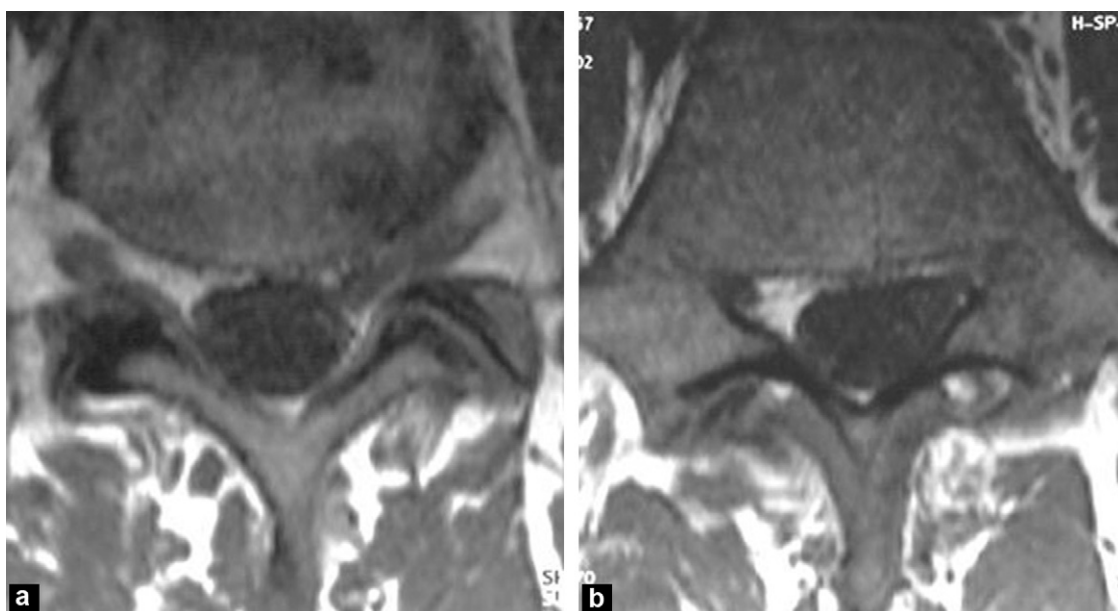


Figure 8. a, b: common L5 and S1 sheath on the left that can simulate left foraminal herniation.



Figure 9. Root cysts in STIR imaging.

failure of the lumbar blood patch procedure, it is necessary to find proof of and locate the CSF leak. Isotopic transit and especially myelography are the most effective techniques for confirming CSF leakage.

Tarlov cysts are found in the sacral region (S1, S2, S3, S4); they are cysts that develop within the dorsal root ganglion, which explains the presence of nerve fibres on the wall of the cyst [12,13]. A CT scan can show enlargement of the sacral canal and/or the anterior foramina, which may simulate a neurinoma. With MRI, a differential diagnosis with a neurogenic tumour can be made owing to the fluid nature of the lesion. Coronal slices, particularly with curved reconstructions, show the intraganglion topography of small cysts

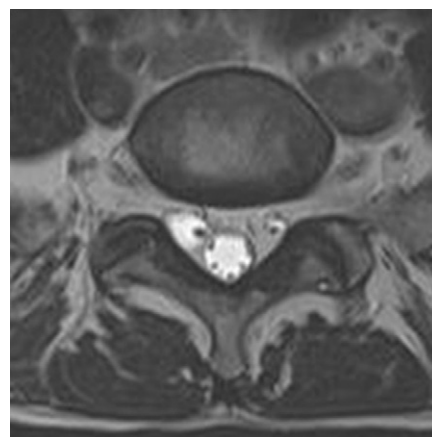


Figure 10. Dilatation of the right S1 root sheath.

and the mass effect on the sacral nerve roots when the cysts are large.

The epidural space

Hypertrophy of the epidural fat associated with endogenous or exogenous hypercorticism, even with simple obesity, can cause stenosis of the lower lumbar or sacral dural sheath. Sagittal and axial T1-weighted images are essential for assessing the degree of stenosis and malformation of the dural sheath [14–16] (Fig. 12). At the level of the thoracic spine, stenosis of the dural sheath caused by the posterior epidural fat should not be confused with an epidural haematoma; this differential diagnosis is sometimes difficult if there is scoliosis, and requires careful analysis of the signal on different sequences, particularly with suppression of the fat signal.

The epidural fat signal appearing heterogeneous (posterior in the thoracic and anterior in the lower lumbar region)



Figure 11. a–c: left S2 and S3 Tarlov cysts.

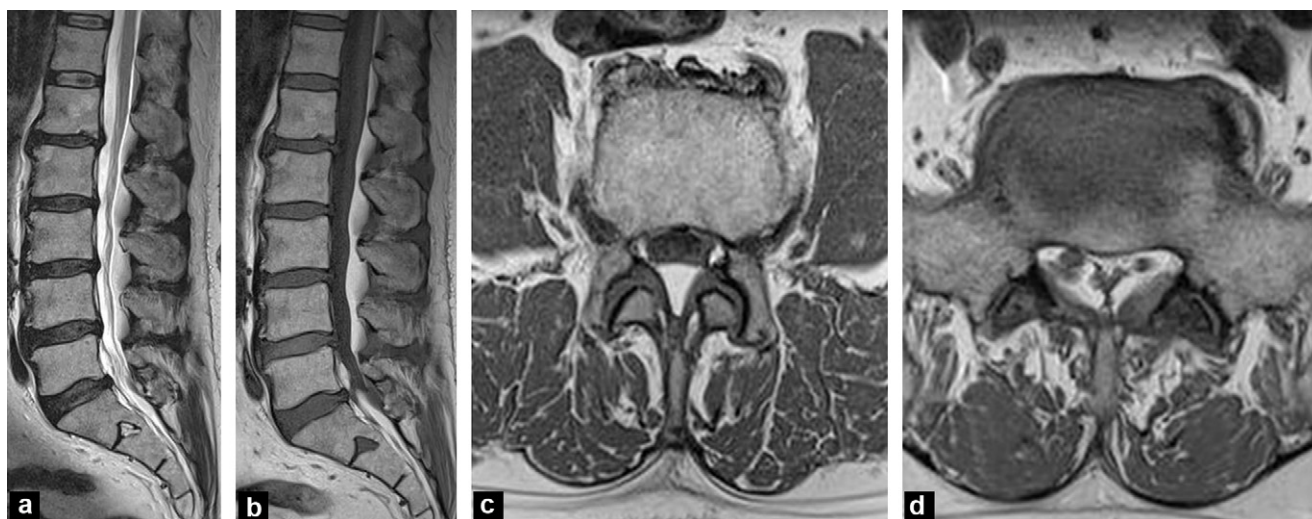


Figure 12. a–d: stenosis of the dural sheath due to fat hypertrophy.

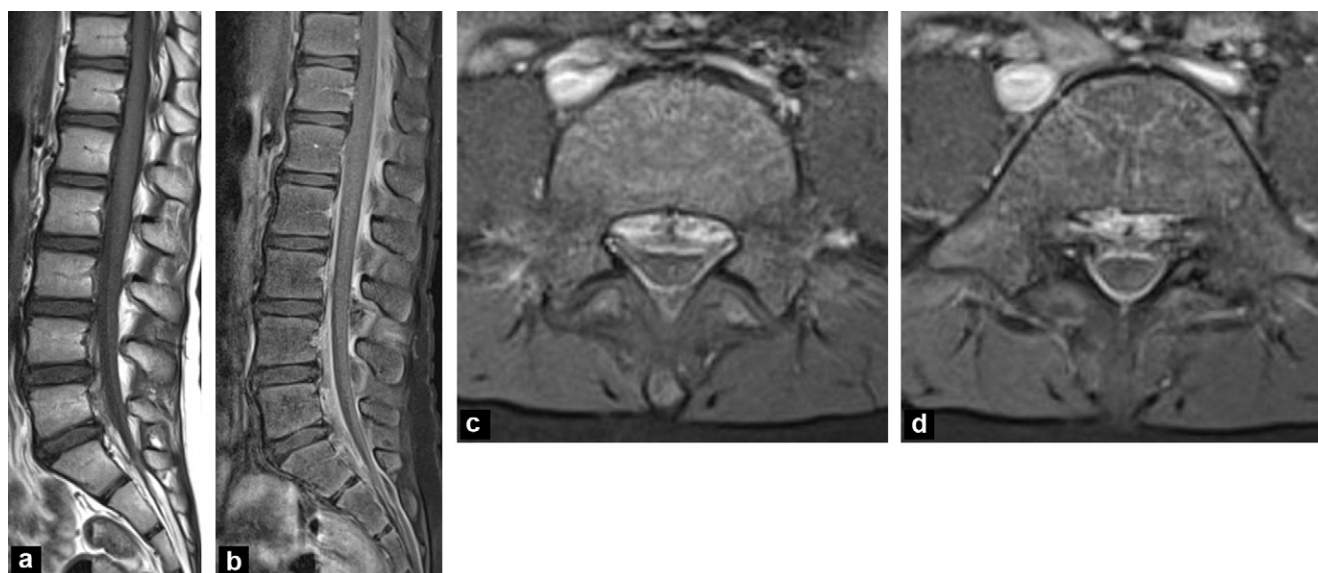


Figure 13. a–d: stenosis of the dural sheath due to dilatation of the epidural veins owing to spontaneous intracranial hypotension.

may indicate epidural vein dilatation or infiltration of the CSF if there is intracranial hypotension, or even tumoral infiltration.

It is difficult to determine the pathogenic nature of an increase in epidural fat; it is often associated with other compression factors (posterior zygapophyseal joint osteoarthritis hypertrophy of the yellow ligaments), which induces clinical decompensation. In the lumbar region, the loss of posterior convexity of the dural sheath and the appearance of concavity on the axial images may indicate pathogenic compression due to increased posterior epidural fat.

Normal epidural veins are identified on axial T1-weighted images after Gadolinium injection. They can be dilated if there is hypotension; the dilatation is then diffuse, but more particularly involves the anterolateral venous plexus at the C1 and C2 levels and the level of the retrocorporeal veins

in the lower lumbar and sacral canal regions [17,18]. Contrast uptake by the dilated veins must not be confused with tumour enhancement. Localised dilatation is usually related to an obstruction within the epidural space; the classic example is venous stasis superjacent and subjacent to disc herniation; this stasis can cause the extent of disc herniation to be overestimated (Fig. 13).

Diffuse dilatation of the epidural veins is also seen when there is thrombosis of the inferior vena cava with development of collateral circulation around the spinal canal [19].

Disclosure of interest

The authors declare that they have no conflicts of interest concerning this article.

TAKE-HOME MESSAGES

- Flow artifacts in the perimedullary CSF are common in T2 spin-echo sequences, particularly in axial slices and uncommon on axial T2 gradient-echo sequences (MEDIC, MERGE, etc.).
- 3D T2-weighted spin echo sequences (SPACE, CUBE etc.) do not allow for a reliable visualisation of intramedullary signal abnormalities.
- T1-weighted MRI images following injection of Gadolinium allow a good visualisation of the veins of the conus medullaris and lumbar root veins.
- If there is stenosis of the lumbar spinal canal, identification of warped roots above or below the stenosis or central displacement of the roots between the levels of compression is likely to indicate a clinically pathogenic stenosis.
- 3D high-resolution T2-weighted imaging is useful for analysing root cysts.
- Diagnosis of an arachnoid cyst or congenital herniation of the spinal cord must be eliminated if there is localised deformation of the spinal cord, particularly in the thoracic region.

References

- [1] Larsen DW, Teitelbaum GP, Norman D. Cerebrospinal fluid flow artifact. A possible pitfall on fast-spin-echo MR imaging of the spine simulating intradural pathology. *Clin Imaging* 1996;20:140–2.
- [2] Fellner C, Menzel C, Fellner FA, Ginthoer C, Zorger N, Schreyer A, et al. BLADE in sagittal T2-weighted MR imaging of the cervical spine. *AJNR Am J Neuroradiol* 2010;31:674–81.
- [3] Monajati A, Wayne WS, Rauschnig W, Ekholm SE. MR of the cauda equina. *AJNR Am J Neuroradiol* 1987;8:893–900.
- [4] Hasegawa T, Mikawa Y, Watanabe R, An HS. Morphometric analysis of the lumbosacral nerve roots and dorsal root ganglia by magnetic resonance imaging. *Spine* 1996;21:1005–9.
- [5] Castillo M, Mukherji SK. MRI of enlarged dorsal ganglia, lumbar nerve roots, and cranial nerves in polyradiculoneuropathies. *Neuroradiology* 1996;38:516–20.
- [6] Coumbaras M, Duval A, Le Hir P, Jomaah N, Arrivé L, Tubiana JM. Fibrolipoma of the terminal filum. *J Radiol* 2003;84:721–2.
- [7] Park HJ, Jeon YH, Rho MH, Lee EJ, Park NH, Park SI, et al. Incidental findings of the lumbar spine at MRI during herniated intervertebral disk disease evaluation. *AJR Am J Roentgenol* 2011;196:1151–5.
- [8] Lane JI, Koeller KK, Atkinson JL. Enhanced lumbar nerve roots in the spine without prior surgery: radiculitis or radicular veins? *AJNR Am J Neuroradiol* 1994;15:1317–25.
- [9] Matge G, Buchheit F, Babin E, Dietemann JL. Congenital anomalies at the emergence of lumbosacral roots. *Neurochirurgie* 1984;30:35–40.
- [10] Song SJ, Lee JW, Choi JY, Hong SH, Kim NR, Kim KJ, et al. Imaging features suggestive of a conjoined nerve root on routine axial MRI. *Skeletal Radiol* 2008;37:133–8.
- [11] Tomoda Y, Korogi Y, Aoki T, Morioka T, Takahashi H, Ohno M, et al. Detection of cerebrospinal fluid leakage: initial experience with three-dimensional fast spin-echo magnetic resonance myelography. *Acta Radiol* 2008;49:197–203.
- [12] Bourgeois P, Gaillard S, Chastanet P, Christiaens JL. Sacral nerve root cysts. Discussion on the mechanism of nerve root suffering. Apropos of 4 cases. *Neurochirurgie* 1997;43:237–44.
- [13] Landers J, Seex K. Sacral perineural cysts: imaging and treatment options. *Br J Neurosurg* 2002;16:182–5.
- [14] Beaujeux R, Dietemann JL, Allal R, Wolfram-Gabel R. Posterior epidural adipose tissue and the narrow lumbar canal: replacement tissue or cause of impingement? *J Neuroradiol* 1995;22:63–70.
- [15] Herzog RJ, Kaiser JA, Saal JA, Saal JS. The importance of posterior epidural fat pad in lumbar central canal stenosis. *Spine* 1991;16(6 Suppl.):S227–33.
- [16] Holl N, Kremer S, Wolfram-Gabel R, Dietemann JL. The spinal canal: from imaging anatomy to diagnosis. *J Radiol* 2010;91(9 Pt 2):950–68.
- [17] Messori A, Polonara G, Salvolini U. Dilation of cervical epidural veins in intracranial hypotension. *AJNR Am J Neuroradiol* 2001;22:224–5.
- [18] Rousset J, Lapierre M, André V, Bellard S, Garcia JF. Dilatation of cervical epidural veins secondary to iatrogenic intracranial hypotension. *J Radiol* 2009;90(1 Pt 1):69–71.
- [19] Paksoy Y, Gormus N. Epidural venous plexus enlargements presenting with radiculopathy and back pain in patients with inferior vena cava obstruction or occlusion. *Spine* 2004;29:2419–24.